N-N one-boson-exchange potentials based on generalized meson field theory

T. Ueda,* F. E. Riewe, and A. E. S. Green
University of Florida, Gainesville, Florida 32611
(Received 14 September 1977)

We present nonrelativistic one-boson-exchange potentials for the N-N interaction by fitting to the most recent N-N phase shifts and deuteron properties. One model makes use of $\pi\pi$ scattering data to characterize the exchange of the ρ meson and the scalar-isoscalar 2π exchange. A second model with the ρ and the scalar-isoscalar component represented by poles is also presented. Reasonable coupling constants and form factor parameters are found and the fit is improved with respect to fits to earlier phase shifts. This tends to confirm the physical meaningfulness of the N-N one-boson-exchange potential model. In addition to this we introduce a model with higher-order velocity-dependent terms which lead to markedly improved fits up to 325 MeV.

[NUCLEAR STRUCTURE Nonrelativistic one-boson-exchange model fit to nucleon-nucleon phase shifts and low-energy parameters.]

I. INTRODUCTION

This paper presents an updated version of our nonrelativistic one-boson-exchange potential (OBEP) approach to the nucleon-nucleon (N-N) interactions on the basis of the recent accumulation of experimental information. Our theoretical basis for this approach is the generalized meson field theory work[1] by one of us (AESG) as well as the early one-boson-exchange model studies[2,3] by one of us (TU), which were successful in the intermediate and outer regions of the N-N interaction. In these 15 years models based upon this approach were brought into quantitative correspondence with phenomenological N-N phase shifts including S waves.[4-6] For these waves, the use of generalized or regularized fields[5] or the equivalent form factors[6] as reinterpreted by Ueda and Green played a critical role. These models lead to smooth velocity-dependent repulsive cores in place of the hard static core of the phenomenological potentials. This feature is not only important for the N-N interaction,[7,8] but also for the N-nuclear interaction.[7]

This regularized OBEP approach was developed further into relativistic versions, first using the Dirac equation[5] and later and more effectively with the Bethe-Salpeter equation.[9] In addition to the work at Florida and Osaka, groups at Texas A&M, M.I.T., Nijmegen, Beer-sheva, Bonn, Paris, and Stony Brook have also pursued similar boson-exchange models. For reviews of these works we refer the reader to Ref. 10 as well as as Refs. 3 and 8.

Further variations of the Florida effort include a relativistic version covering the inelastic region.[11] An isoscalar-scalar meson σ with mass 400–600 MeV is used in the models. The meson has been interpreted as representing the $I=J=0$ part of the two-pion exchange.[12] In this respect, models with σ replaced by the experimental $\pi\pi$ scattering phase shift contributions were also presented.[7,13,14]

Recently, Arndt, Hackman, and Roper (AHR)[15] have presented reanalyses of the phase parameters based on accumulation of new data which should increase the accuracy, compared with the parameters available 10 years ago.[16,17] The new error bars of the phase parameters are approximately one-half of the old ones. More recently important experimental data and analyses have become available between 0–515 MeV.[18-22] These studies have exposed additional defects in the old phase parameters. For example, the D_t parameter data of n-p scattering at 325 MeV, provided by recent measurements at TRIUMPH[18] deviate considerably from the prediction of the Livermore X solution.[17] In addition new measurements of the A_{yy} parameter for n-p scattering at 50 MeV have led to the conclusion that the ϵ_1 parameter should be positive in this energy region,[20] although the ϵ_1 parameter given in the Livermore analyses has been persistently negative. Since most potentials, either theoretical or phenomenological, have been constructed with reference to the old phase parameters, especially the Livermore X solution, we believe that it is worthwhile to present new potentials based on the new data.

Besides updating our nonrelativistic potentials we here introduce new potentials with higher-order velocity-dependent terms. With three parameters describing these terms we show remarkable improvements by removing some deviations which have appeared persistently in some states between

250–325 MeV. Potentials obtained in this paper provide simple and good descriptions of the nucleon-nucleon interactions up to 325 MeV with 11 to 12 parameters. The new potentials have manifest improvements over the last nonrelativistic potentials.[14] For example they have the χ^2 values of $\frac{2}{3}$–$\frac{1}{2}$ of the old ones.

In Sec. II we define the OBEP used in this paper. In Sec. III a revised version of the OBEP with realistic ρ and scalar-isoscalar 2π exchange is presented. The contributions to the potential are obtained from experimental $\pi\pi$ scattering phase shifts.[23] In Sec. IV a revised version of the OBEP with σ (scalar-isoscalar) and ρ represented by two poles and one pole, respectively, is presented. In Sec. V we introduce the higher-order velocity-dependent terms into the model of Sec. IV. Section VI gives our discussions and conclusions.

II. OBEP

The OBEP were derived in the literature by Green and Sawada[5] and Ueda and Green.[6] We show these OBEP in Table I. They are correct through the order of p^2/M^2, where p is the magnitude of the three-momentum of any nucleon in c.m. system, M is the nucleon mass, μ is the meson mass, and Λ is the parameter of the form factor for the meson-nucleon vertex:

$$F(k^2)=\left(\frac{\Lambda^2}{k^2+\Lambda^2}\right)^N . \tag{1}$$

For isovector mesons, the potentials should be multiplied by $\vec{\tau}_1\cdot\vec{\tau}_2$.

We write the total OBEP as a sum of the velocity-independent terms and the velocity-dependent ones as, i.e.,

$$(\text{total OBEP})=V(r)-\frac{1}{2M}[\nabla^2\phi(r)+\phi(r)\nabla^2], \tag{2}$$

where $\phi(r)$ has the following expression:

$$\phi(r)=\frac{1}{M}\sum_i g_i^2 Y(\mu_i,\Lambda_i) . \tag{3}$$

In this equation $\sum$ implies a summation over mesons contributing to the velocity-dependent terms, that is, scalar and vector mesons in the present case, and $Y(\mu_i,\Lambda_i)$ is the modified potential function in Table I. After a transformation of the radial wave function $u(r)$ for the Schrödinger equation,

$$\frac{\psi(r)}{[1+\phi(r)]^{1/2}}=u(r) , \tag{4}$$

we have the ordinary form of the Schrödinger equation for $\psi(r)$;

$$\psi''(r)-\frac{l(l+1)}{r^2}\psi(r)+(p^2-M)V_{\text{eff}}(r,p^2)\psi(r)=0 , \tag{5}$$

where $V_{\text{eff}}(r,p^2)$ is the effective potential given by

$$V_{\text{eff}}(r,p^2)=\frac{V(r)}{1+\phi(r)}-\frac{1}{4M}\left(\frac{\phi'(r)}{1+\phi(r)}\right)^2+\frac{p^2}{M}\frac{\phi(r)}{1+\phi(r)} . \tag{6}$$

TABLE I. One boson-exchange potential.

$$V_{\text{psc}}(r)=g_{ps}^2\left(\tfrac{1}{6}Y^{(2)}\vec{\sigma}_1\cdot\vec{\sigma}_2+ZS_{12}\right),$$

$$V_{\text{scl}}(r)=g_s^2\left[-Y+\tfrac{1}{2}Y^{(2)}-\frac{1}{2M^2}(\nabla^2Y+Y\nabla^2)+Y^{(1)}\vec{L}\cdot\vec{S}\right],$$

$$V_{\text{vec}}(r)=g_v^2Y+g_v^2(1+f_v/g_v)Y^{(2)}-g_v^{(2)}\frac{1}{2M^2}(\nabla^2Y+Y\nabla^2)+g_v^2(1+f_v/g_v)^2\tfrac{1}{3}Y^{(2)}\vec{\sigma}_1\cdot\vec{\sigma}_2-g_v^2(1+f_v/g_v)^2ZS_{12}$$

$$+g_v^2(3+4f_v/g_v)Y^{(1)}\vec{L}\cdot\vec{S},$$

$$Y=\left(\frac{\Lambda^2}{\Lambda^2-\mu^2}\right)^2\frac{1}{r}\left(e^{-\mu r}-e^{-\Lambda r}\left\{1+\frac{\Lambda^2-\mu^2}{2\Lambda}r\right\}\right), \quad \text{for } N=1,$$

$$Y=\frac{1}{\tau^4 r}\left[e^{-\mu r}-e^{-\Lambda r}\left\{1+\frac{\tau}{2}+\frac{\tau^2}{8}+\frac{\tau^3}{16}\Lambda r+\frac{\tau^2}{8}+\frac{\tau^3}{16}(\Lambda r)^2+\frac{\tau^3}{48}(\Lambda r)^3\right\}\right],$$

with $\tau=(\Lambda^2-\mu^2)/\Lambda^2$, for $N=2$.

$$Y^{(1)}=\frac{1}{2M^2}\frac{1}{r}\frac{dY}{dr}, \quad Y^{(2)}=\frac{1}{2M^2}\langle\nabla^2Y\rangle, \quad Z=\frac{1}{4M^2}\left(\frac{1}{r^2}+\frac{\mu}{r}+\frac{\mu^2}{3}\right)Y;$$

$$S_{12}=3\frac{\vec{\sigma}^1\cdot\vec{r}\,\vec{\sigma}^2\cdot\vec{r}}{r^2}-\vec{\sigma}^1\cdot\vec{\sigma}^2, \quad \vec{L}\cdot\vec{S}=\tfrac{1}{2}(\vec{\sigma}^1+\vec{\sigma}^2)\vec{L},$$

where ∇^2 operates on all functions to the right.

III. OBEP USING $\pi\pi$ DATA

Our overall goal is to produce an accurate OBEP model in which all parameters are determined directly from experiment. At present, meson-nucleon coupling constants and form factors are not known accurately enough to be used directly, and are taken to be adjustable parameters. In earlier models[4-7] the $I=J=0$ part of the 2π exchange, which is the sum of the uncorrelated and correlated 2π exchange, is approximated by the isoscalar-scalar meson σ with the mass and the coupling constant adjusted.

In more recent models,[8,13,14] $\pi\pi$ scattering data have been used in place of the σ meson. The approach we will use at present is that followed by Riewe, Nack, and Green[14] as described below. We will present a number of OBEP calculations in this section. Some are given to show how changes in phase-shift data have affected the OBEP models, while others represent a best fit of a model to the latest data. Our basic OBEP model uses the π, η, ω, ρ, and δ mesons, with the ρ meson treated as a resonance. Both the ρ meson and the $\pi\pi$ S-wave $I=0$ contributions to the OBEP are obtained from $\pi\pi$ scattering data with only their form factors and coupling constants taken to be adjusted parameters. All mesons (including the $\pi\pi$ S waves) are assumed to have meson-nucleon form factors given by Eq. (1) with $N=2$. This is the same functional form as the experimentally determined electron-proton form factor.[24]

For the ρ meson and $\pi\pi$ S waves we use the formalism developed by Nack, Ueda, and Green[13] and used by Riewe, Nack, and Green (RNG).[14] For both the ρ and $\pi\pi$ cases, the contribution to the N-N potential is of the form

$$J(r,\Lambda)=\int_{a_r}^{b_r} Y(r,\Lambda,t')\rho^{\ell}(t')dt', \tag{7}$$

where the spectral function $\rho^{\ell}(t')$ is given by

$$\rho^{\ell}(t')=\frac{\mathrm{Im}\bar{\Delta}^{\ell}(t',\Gamma)}{I^{\ell}}, \tag{8}$$

$$\mathrm{Im}\bar{\Delta}^{\ell}(t',\Gamma)=\frac{t_r\Gamma_l^{\,2}(t')}{(t_r-t')+t_r\Gamma_l^{\,2}(t')}, \tag{9}$$

$$\Gamma_l(t')=\Gamma_r\left[\left(\frac{t'-a_r}{t_r-a_r}\right)\left(\frac{b_r-t'}{b_r-t_r}\right)\right]^{l+1/2}, \tag{10}$$

$$I_{\ell}=\int_{-\infty}^{\infty}\mathrm{Im}\bar{\Delta}^{\ell}(t',\Gamma)dt'. \tag{11}$$

The potential function $Y(r,\Lambda,t')$ is obtained from Table I by replacing μ with $(t')^{1/2}$. The resonance parameters (t_r,Γ_r,a_r,b_r) are fitted to $\pi\pi$ data as in RNG, with the Baton solution[25] used for the ρ and the "down" solution[25] used for the S-wave contribution. The parameters are given in Table II.

TABLE II. Calculated $\pi\pi$ scattering parameters.

δ_l^I	t_r (GeV^2)	Γ (GeV)	a_r (GeV^2)	b_r (GeV^2)
δ_0^0	0.748	0.500	0.0770	1.00
δ_1^1	0.585	0.135	0.0770	1.69

As previously discussed, the phase-shift data of MacGregor, Arndt, and Wright[17] (MAW) have been superseded by an analysis by Arndt, Hackman, and Roper[15] (AHR). An updated version of the AHR data has been presented by Arndt.[22] Our first order of business is to determine what implications the newer results have for OBEP models. We will consider only the energy-independent phase-shift data to avoid being influenced by the OPEP parametrization used in the energy-dependent data. The model is fitted to data for $J\leq 2$ at 6 energies from 25 to 325 MeV by adjusting 11 parameters: $g_\pi^{\,2}$, $g_\eta^{\,2}$, $g_\omega^{\,2}$, $g_\rho^{\,2}$, $g_\delta^{\,2}$, $g_{\pi\pi}^{\,2}$, f_ρ/g_ρ, Λ_π, Λ_ρ, $\Lambda_{\pi\pi}$, and $\Lambda_\eta=\Lambda_\omega=\Lambda_\delta$. For MAW, we obtain $\chi^2=274$, or $\chi^2/d=3.97$ for $d=69$ data. If we substitute phase-shift data from AHR, but keep the same error bars as in MAW, readjustment of parameters yields $\chi^2/d=3.80$. Thus our model is somewhat more compatible with the AHR data than with MAW. Using both data and error bars from AHR gives $\chi^2/d=10.3$ due to the increased accuracy of the data.

A similar comparison may be made between AHR and the update by Arndt. Using Arndt data and AHR error bars ($d=68$ data) the value of χ^2/d drops to 8.41, indicating much closer agreement. This strongly suggests that our OBEP model is fundamentally correct and that as the experimental data are refined, they become more consistent with our model.

We now present models fitted to the Arndt phase-shift parameters and error bars. Model I is the same model used above, but fitted to the 68 Arndt data with $\chi^2/d=11.3$. The phase shifts are shown in Fig. 1 and potential parameters are given in Table III. The only parameters which changed more than 20% from fits to the MAW data are Λ_π, which more than doubled, and $g_\delta^{\,2}$, which increased by a factor of 6. Neither of these has a strong effect on the resulting potential. Λ_π is expected to be high, because of the lack of isovector pseudoscalar mesons to contribute to the pion form factor. The present model is also fitted to the combined data described in the Appendix with the result $\chi_C^2/d=8.6$, when the parameters are readjusted to fit for the energy range of 25–325 MeV, irrespective of the low-energy and deuteron parameters.

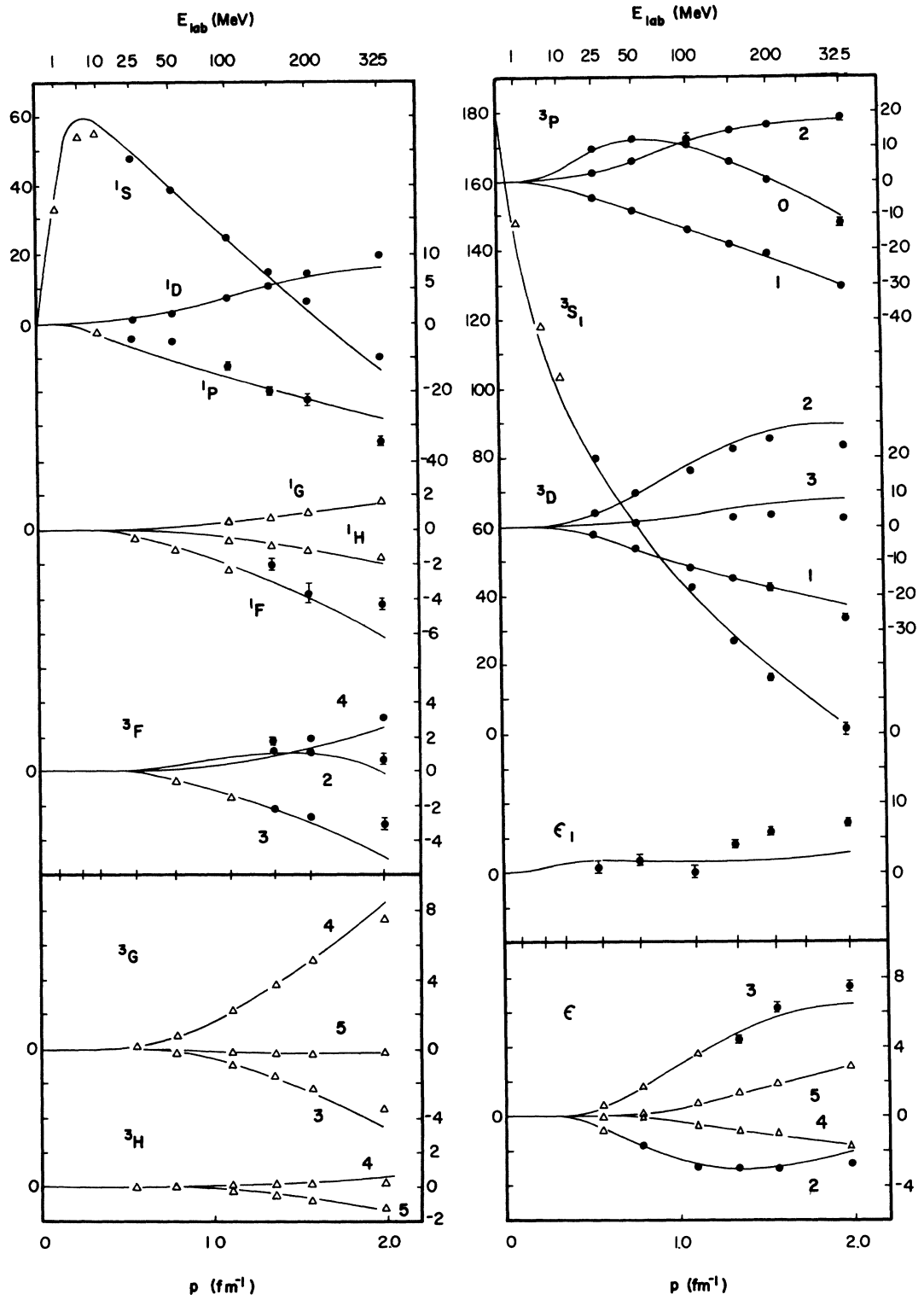

FIG. 1. Phase parameters for model I. The upper scale is incident energy (MeV) in the laboratory system and the lower scale is the incident momentum (fm^{-1}) in the c.m. system. Circles indicate the energy-independent data of Arndt (Ref. 22), which differs from AHR (Ref. 15) only at 50 and 325 MeV. Where energy-independent data are not available, energy-dependent data of AHR are plotted as triangles. Shown are the p-p phase parameters.

TABLE III. Model parameters. χ^2_A denotes the total χ^2 for 68 energy-independent data by Arndt (Ref. 22). χ^2_C denotes the total χ^2 for 72 combined data of AHR (Ref. 15), Arndt (Ref. 22), Signell (Ref. 21), and Edgington (Ref. 18). χ^2_{AHR} denotes the total χ^2 for the 72 data of the energy-dependent solution of AHR (Ref. 15) as described in the Appendix. χ^2_L includes 19 data at 1 and 5 MeV with error bars set equal to 0.1. Fixed parameters are denoted by an asterisk (*). The parameters Ω_0 and Ω_1 in model III are defined in Eq. (14).

Model (number of parameters)	Meson	g^2	f/g	μ (MeV)	Λ (MeV)	χ^2/datum (fitted energy region)
I	π	13.94		138.7*	4216.4	
(11)	η	6.49		548.7*	1845.8	$\chi^2_A/d = 11.3$
	ω	11.86	0.0	782.8*	1845.8	
	ρ	0.357	7.49		1288.9	
	δ	2.51		963.0*	1845.8	(25–325 MeV)
	$\pi\pi$	10.88			1445.9	
I′	π	13.96		138.7*	3738.3	
(11)	η	5.50		548.7*	1836.4	$\chi^2_A/d = 13.3$
	ω	11.03	0.0	782.8*	1836.4	(0–325 MeV)
	ρ	0.381	7.10		1309.2	
	δ	2.31		963.0*	1836.4	$\chi^2_L/87 = 10.8$
	$\pi\pi$	10.39			1459.7	
II	π	14.24		138.7*	2012.0	
(12)	η	5.77		548.7*	1129.5	$\chi^2_C/d = 10.4$
	ω	10.06	0.0	782.8*	1129.5	(0–200 MeV)
	δ	2.64		970.0*	1129.5	
	ρ	0.71	4.94	759.1*	1000.0	
	σ	3.16		484.3	1129.5	
	S*	6.78		993.0*	1129.5	
II′	π	13.25		138.7*	2339.1	
(12)	η	7.63		548.7*	1120.5	$\chi^2_{AHR}/d = 9.7$
	ω	8.67	0.0	782.8*	1120.5	
	δ	2.51		970.0*	1120.5	(0–325 MeV)
	ρ	0.659	4.80	708.6	1120.5	
	σ	3.07		484.3	1120.5	
	S*	4.62		993.0*	1120.5	
III	π	13.26		138.7*	3171.9	
(12)	η	7.40		548.7*	1221.4	$\chi^2_C/d = 6.8$
	ω	11.20	0.0	782.8*	1221.4	(0–325 MeV)
	δ	5.80		970.0*	1221.4	
	ρ	1.45	2.93	759.1*	1221.4	
	σ	4.12		477.9*	1221.4	
				$\Omega_0 = -79.6$ MeV, $\Omega_1 = 322$ MeV, $\kappa = 200$* MeV		

Deuteron parameters may be calculated as described by Gersten and Green.[26] To improve the low-energy properties of the model, we add the AHR energy-dependent phase shifts at 1 and 5 MeV, with error bars arbitrarily set equal to 0.1°. A fit gives $\chi^2/d = 13.3$ for the original 68 data. The resulting parameters are presented as model I′ in Table III and the low-energy properties are given in Table IV. The phase shifts do not change noticeably from those in Fig. 1.

Models I and I′ show specific improvements over previous calculations. In particular there is better agreement with the 50 MeV data, and the $^1P_1$, which has always been troublesome, is much improved. However, certain systematic deviations from the experimental data are apparent in Fig. 1. In particular, the fit can be improved considerably by slight adjustments in the $^1S_0$, $^3S_1$, $^1P_1$, and $^3D_2$ phase shifts. These inaccuracies in the model were not nearly so apparent with earlier data. It is clear that the increased precision of the data will allow us to test additional ingredients in the OBEP model, as will be done in Sec. V. In Sec. IV, we will relax the condition that the ρ and $\pi\pi$ contributions are related with experimental $\pi\pi$ scattering data.

TABLE IV. Deuteron and low-energy parameters.

	Experiment		I′	II	II′	III
Deuteron binding energy (MeV)	2.224 52 (1 ± 0.000 09)		2.27	2.23	2.16	2.16
$^3S_1$ scattering length (fm)	5.399	±0.011	5.86	5.46	5.49	5.43
$^3S_1$ effective range $\rho(-\epsilon,-\epsilon)$ (fm)	1.82	±0.05	1.83	1.82	1.78	1.73
D state probability (%)			4.84	5.04	4.58	6.37
Quadrupole moment (10^{-27} cm)	2.82	±0.01	2.60	2.71	2.55	2.63
Magnetic moment (μ_N)	0.857 41	±0.000 08	0.85	0.856	0.861	0.851
$^1S_0$ scattering length (fm)	−23.675	±0.095	−17.1	−23.7	−28.3	−24.6
$^1S_0$ effective range (fm)	2.69	±0.18	2.87	2.78	2.71	2.79

IV. OBEP WITH THE POLE ρ AND THE POLE σ

A. Models II and II′

The ingredients in these models are π, η, ω, ρ, δ ($I=1, J^P=0^+$), σ ($I=0$, $J^P=0^+$), and S^* ($I=0, J^P=0^+$).

Since there are possible contributions to the $I=J=0$ exchange (1) from uncorrelated two-pion exchange which is not related with the $\pi\pi$ scattering phase shifts and (2) from exchanges of heavy bosons not explicitly treated here and there are considerable uncertainties in two-pion-exchange theory available at present, we have the advantage of including all possible effects in our phenomenological treatment of the isoscalar-scalar component.

Models II and II′ represent the isoscalar-scalar component by two poles, σ and S^*. S^* is now an established meson with a mass of 993 MeV. The mass of σ is searched. ρ is also represented by one pole whose mass is fixed to the observed value in model II, while searched in model II′. In these models the form factor with $N=1$ in Eq. (1) is used. Model II has 12 parameters of g_π^2, g_η^2, g_ω^2, g_ρ^2, f_ρ/g_ρ, g_δ^2, $g_{S^*}^2$, g_σ^2, m_σ, Λ_π, Λ_ρ, and Λ in common for the remaining mesons. These parameters are adjusted to make fits to the combined data of AHR, Arndt, and Signell described in the Appendix at 25, 50, 100, 150, and 200 MeV as well as the low-energy and deuteron parameters. Considering the nonrelativistic approximation in our potential, we delete the data at 325 MeV to minimize the χ^2 value. In this model we get $\chi^2_C/\text{data}=10.4$ for the 25–200 MeV data and $\chi^2_C/\text{data}=11.9$ for the 25–325 MeV data. The fits to the low-energy and deuteron parameters have approximately in a 1% error.

Model II′ has 12 parameters of g_π^2, g_η^2, g_ω^2, g_ρ^2 f_ρ/g_ρ, g_δ^2, $g_{S^*}^2$, g_σ^2, m_σ, m_ρ, Λ_π, and Λ in common for the remaining mesons. These parameters are adjusted to the energy-dependent solution of the phase parameters given by AHR at 25, 50, 100, 150, 200, and 325 MeV as well as the low-energy and deuteron parameters. In this model we get $\chi^2_{\text{AHR}}/\text{data}=9.7$. This is better than that of model II. However, fits to the low-energy and deuteron parameters are not precise enough for the deuteron quadrupole moment and the low-energy parameters in the $^1S_0$ state.

B. Fits

Figure 2 shows comparisons of the results in these models with those of AHR, Edgington *et al.*, and Signell *et al.* Broken and dotted curves show results in model II and II′, respectively. Approximately $\frac{2}{3}$ of the total χ^2 comes from fits in the $^3D_2$, $^3S_1$, $^1S_0$, and $^1D_2$ states at 200–325 MeV in models II and II′. The deuteron and low-energy parameters are calculated with the Gersten-Green code.[26] They are shown in Table III.

Considering that we ignored terms of the order $(p/M)^4$ in the potentials in Table I, and contributions from bosons with mass larger than 1000 MeV, we think that models II and II′ are quite reasonable with some sacrifice in the high energy fits.

C. Coupling constants

We obtained 14.2 and 13.3 for g_π^2 in models II and II′, respectively. These are smaller than that used in AHR where $g_\pi^2=15$. However, the fits to the high partial waves with $3\leq J\leq 5$ are satisfactory. g_ω^2 and f_ω/g_ω are 10-8.7 and 0, respectively, g_ρ^2 and f_ρ/g_ρ are 0.71-0.66 and 4.9-4.8, respectively, in model II and II′. They are reasonable in comparison with results of analyses of the electromagnetic form factor[27]:

$$g_\rho^2=0.52^{+0.07}_{-0.06},\quad g_\omega^2=4.69,\quad g_\phi^2=3.04^{+1.07}_{-0.66},\quad f_\rho/g_\rho=3.6,\quad f_\omega/g_\omega=0. \tag{12}$$

The larger values of g_ρ^2, f_ρ/g_ρ, and g_ω^2 in models

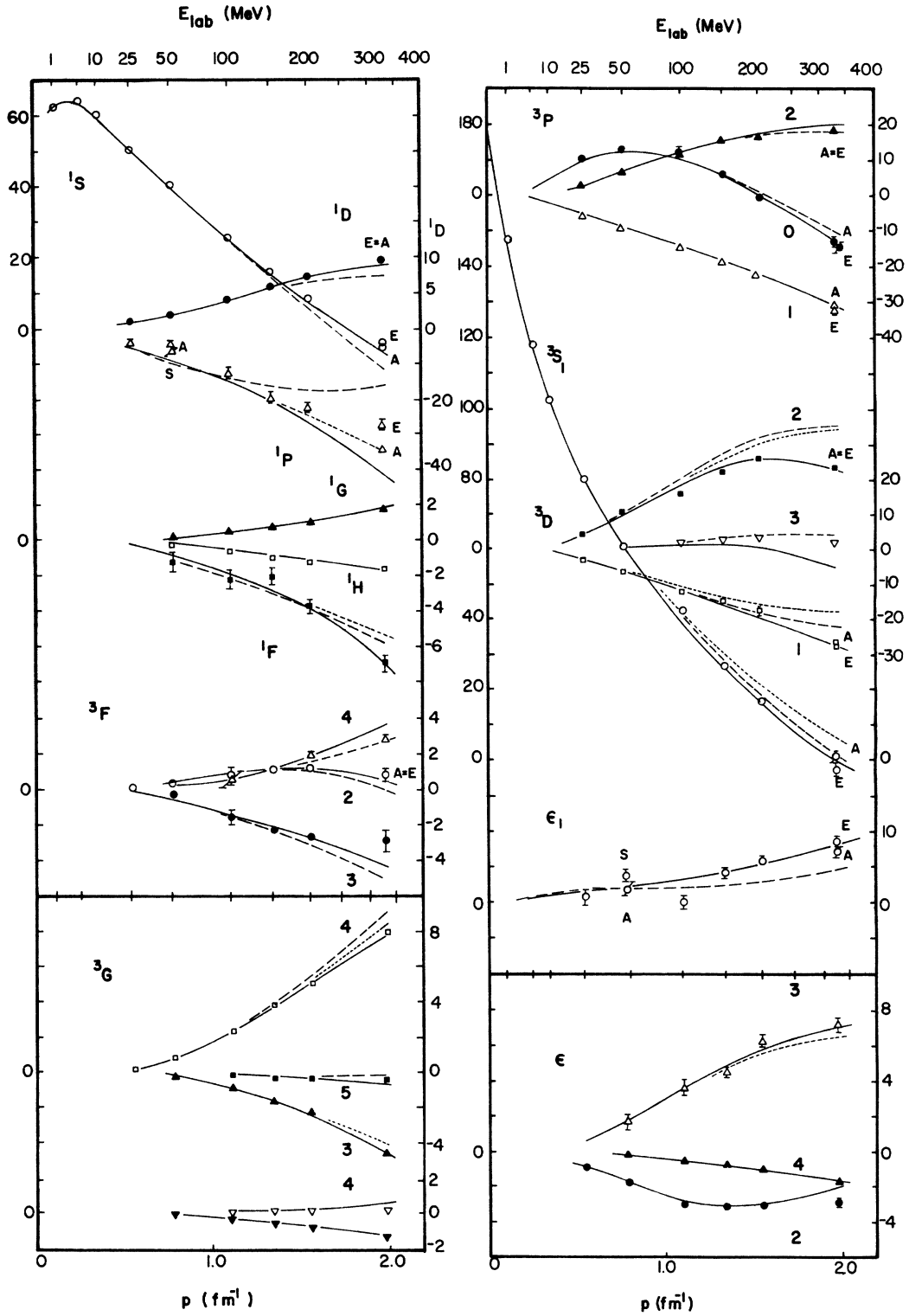

FIG. 2. Phase parameters versus incident energy (MeV) in the laboratory system (upper scale) and incident momentum (fm^{-1}) in the c.m. system (lower scale). Solid, broken, and dotted curves represent calculations of models III, II, and II′, respectively. Phase parameters of model II, (II′) which are not much different from those of III (II) are not plotted. The data are from AHR except those denoted by A, E, and S. A, E, and S denote the data of Arndt (Ref. 22), Edgington (Ref. 18), and Signell (Ref. 21), respectively. Shown are the n-p phase parameters.

II and II′, compared with the above ones may be interpreted such that these models involve the uncorrelated 2π and 3π exchanges with do not correspond to the electromagnetic form factor.

We obtain rather large g_η^2 in models II and II′, approximately 6–8. g_η^2 has often been reported to be small as $g_\eta^2 \lesssim 0.002$ from analyses of other reactions.[28] If this is true, the η contribution here may represent some part of the $I=J=0$ three-pion exchange contribution and/or η' (958 MeV).

D. Deviations from the data at 325 MeV

We obtained considerably smaller values for ϵ_1 and more positive values for $\delta(^3S_1)$ at 200–325 MeV, compared with the data. Perhaps the two deviations of ours from the data are correlated, since the tensor force in the $^3S_1$-$^3D_1$ states reflecting most in the ϵ_1 parameter produces an attractive central force in the second-order process, and this is balanced against the repulsive central force existing more inside.

Regarding that the deuteron quadrupole moment in model II′ is 2.6 and smaller than the experimental value 2.8, the tensor force in model II′ may be somewhat weaker than that required by experiment. A larger value for the ϵ_1 parameter of about 6° at 325 MeV would bring the exact fit of the quadrupole moment to the experimental value. Actually, this was the case in the OBEP by Ueda and Green (UGI),[6] where ϵ_1 fits completely the data of Breit *et al.* which has $\epsilon_1 = 6°$ at 325 MeV[16] and the quadrupole moment agrees exactly with the experimental value.

Considerable deviations of the present results from the data are seen at 200–300 MeV in the $^1D_2$ and $^3D_2$ states. We think that causes for the deviations are in the nonrelativistic approximation of the potentials. Including the terms of the order $(p/M)^4$, we may have potentials of the type L^2 and $\vec{\sigma}^1 \cdot \vec{L}\vec{\sigma}^2 \cdot \vec{L}$. Ueda and Green have shown that to introduce these types of potentials reduces the deviations[6,7] considerably. The effect of the higher-order velocity-dependent terms is discussed in the next section.

E. Deuteron, triton, and nuclear matter

In model II we have satisfactory fits to deuteron properties. The models II and II′ give a D-state probability of 5.0 and 4.5%, respectively. These values are considerably smaller than those of other phenomenological potentials, for example, 6.97% of the Hamada-Johnston potential. In this context we note here that a recent analysis of $\pi^+ d \to pp$ has given 4% for the D-state probability.[29]

The triton's binding energy is experimentally 8 MeV. This value is hard to reproduce by those potentials which give a D-state probability of ~7%. Actually these potentials give less binding by 1–2 MeV. It is known that a potential giving less D-state probability can produce more binding in tritons.[30] Thus our potential of model II as well as II′ would have some advantage in the triton binding energy calculation though there is some uncertainty of the three-body forces contribution to the binding energy.

In comparison with the Ueda-Green potential (UGI) which gives 5.5% of the D-state probability and produces saturation in nuclear matter with binding energy of 14 MeV at $k_F = 1.6$ fm^{-1},[31] the potentials of models II and II′ with less D-state probability would give a saturation with more binding energy at a higher density. However, we emphasize here that a simple comparison of a two-body force contribution to nuclear matter binding energy with the experimental data (the saturation with 16 MeV binding energy at $k_F = 1.36^{-1}$)[32] does not lead to real understanding. Ueda, Sawada, and Takagi have recently shown that there are considerable contributions from three-body forces due to heavy bosons and that two-body forces themselves change in nuclear matter at high densities.[33,34]

V. OBEP WITH THE HIGHER-ORDER VELOCITY-DEPENDENT TERMS

In this section we study the OBEP with higher-order velocity-dependent terms. The potentials in Table I do not involve the terms of the order $(p/M)^4$. This would be the primary reason for the deviations at 325 MeV. We supplement model II by introducing higher-order velocity-dependent terms into the effective potentials of Eq. (6) as follows:

$$\tilde{V}_{\text{eff}}(r,p^2) = \frac{V(r)}{1+\phi(r)} - \frac{1}{4M}\left(\frac{\phi'(r)}{1+\phi(r)}\right)^2 + \frac{p^2}{M}\frac{\phi(r)}{1+\phi(r)}[1+H(p^2)], \tag{13}$$

where we assume the function modifying the p^2 term as

$$H(p^2) = \frac{p^2}{\Omega|\Omega|}\,\frac{1}{1+p^2/\kappa^2}. \tag{14}$$

In Eqs. (13) and (14) p^2 is given by $p^2 = E_{\text{lab}} M/2$ where E_{lab} is incident nucleon energy in the laboratory system. We use three parameters for $H(p^2)$, Ω_0, and Ω_1 for the $I=0$ and $I=1$ states, respectively, and κ in common for both states. κ is fixed to be 200 MeV. This assures no singularity at the normal nuclear density. For example, the binding energies of deuteron and nuclear matter,

2.2 and 16 MeV, respectively, correspond to $p^2 = -(45\ \mathrm{MeV}/c)^2$ and $-(123\ \mathrm{MeV}/c)^2$. We take κ to be large compared with these values.

In this study we use π, ρ, ω, δ, σ, and η without mass distributions. We deleted S^* for simplicity and since we found only a minor contribution from S^* in the search procedure for fitting. Thus we adjust the 12 parameters: g_π^2, g_ρ^2, f_ρ/g_ρ, g_ω^2, g_δ^2, g_σ^2, g_η^2, m_σ, Λ_π, Λ, Ω_0, and Ω_1. The parameter Λ is used in common for all mesons except the pion. The meson masses other than σ are fixed at the observed values.

Numerical results are shown in Table II and IV and Fig. 2. We find that the higher-order velocity-dependent terms required for the overall fits are repulsive for the $I=0$ states and attractive for the $I=1$ states. With these terms we can satisfactorily remove the five deviations in models II and II′ at 200–325 MeV, i.e., those in the $^1D_2$, $^1S_0$, $^3S_1$, $^3D_2$, and ϵ_1 parameters. Thus we have a much reduced χ^2 value, $\chi_C^2/\mathrm{data} = 6.8$.

This potential has now a different character from model II or II′ as follows:

(i) The velocity-dependent repulsion in the $I=1$ states increases more weakly with energy than that in model II or II′.

(ii) The velocity-dependent repulsion in the $I=0$ states increases more strongly with energy than that in model II or II′.

(iii) The tensor component of the potential in the $I=0$ states is now stronger than that of model II. This stronger tensor component may produce a stronger attractive central force and balance against the stronger velocity-dependent repulsion mentioned in (ii). The stronger tensor component results in a large D-state probability, 6.4%, compared with those of models II and II′, 5.0 and 4.5%, respectively. This is clearly an area for improvement in future models.

VI. DISCUSSION AND CONCLUSIONS

A. Relationship with the relativistic works

We next compare the present results with our relativistic works[9,11,35] in which the scattering problem was solved in momentum space and relativistic energy-momentum relations were used for the two-nucleon propagator and the potential derivation. As a companion work to this paper we have made an updated version[35] of the relativistic potential which has much improved fits with $\chi_C^2/\mathrm{data} = 7.4$ and good fits to the low-energy parameters over the older works.[11] In addition to this we introduced asymptotic energy-dependent factors into the vector and scalar potentials, which are in accord with requirements of high-energy physics. This reduced markedly the χ_C^2 value to $\chi_C^2/\mathrm{data} = 4.6$ with only one more parameter involved. Those relativistic potentials give satisfactory descriptions of the nucleon-nucleon interactions up to 515 MeV. The relativistic treatment apparently has the advantage of including the higher-order terms than $(p/M)^2$ which are ignored in models I, I′, II, and II′. However, a comparison of the present fits in these models with those in our relativistic work below 200 MeV indicates that the difference is not large. The major part of the higher-order terms seems to be absorbed in relatively minor parameter adjustments of the nonrelativistic version. However, we should note that in the relativistic work (in Ref. 35), the problem in the $^3D_2$ phase shift at 325 MeV which is persistent in our nonrelativistic versions is almost removed. An advantage of the nonrelativistic potentials is to provide an intuitive picture of nuclear forces and to give a familiar basis for nucleus problems.

It has been conjectured that the velocity-dependent repulsive core associated with the OBEP may be too soft. However, since our relativistic work covering the inelastic energy region up to 515 MeV[35] showed that the relativistic potential can reproduce correctly the $^1S_0$ phase shift up to 515 MeV and since the present nonrelativistic result has a good correspondence with the relativistic one in all phase parameters up to 200 MeV, we believe that the velocity-dependent core pictured in this nonrelativistic version is realistic from a physical viewpoint.

B. s-dependent form factor and the velocity-dependent potential

Recently, Holinde and Machleidt[36] have presented an OBE model in momentum space with an incident-energy-dependent form factor. Though their fits are to the 1969 Livermore phase parameters,[17] the fits appear quite good. Since there are considerable changes in the new result by AHR,[15] Arndt,[22] Signell,[21] and Edgington[18] from the old Livermore phase parameters, some readjustment of their parameters is needed. The form factor employed by them is characteristic. It is derived in an eikonal formalism of multiple exchange of vector mesons, but includes a phenomenological parameter. It is interesting that the form factor depends on the incident energy ($\sqrt{s}$) as well as the momentum transfer.

In connection with the s dependence of the form factor, we might note the following. One of us (TU) made a model[37] where a bilocal field is exchanged and this corresponds to the exchange of an infinite series of mesons with various spins. This scheme could be adapted so that the model reduces to the OBE model at low energies, while

it tends to the Regge-pole model producing the s dependence at high energies. We think that this is a possible direction for extension of our OBEP, especially in momentum space. Actually we have introduced into the relativistic potentials[35] the asymptotic energy-dependent factor which satisfies the requirements for the OBE model at low energies and for the Regge-pole model at high energies, and obtained much improved results. On the other hand, we note in the nonrelativistic version in this paper that the higher-order velocity-dependent terms in model III may be interpreted to involve in part the modification due to the asymptotic energy-dependent factor as well as the relativistic corrections.

C. Conclusions

In this paper we have provided simple and physically reasonable descriptions of the nucleon-nucleon interaction below 325 MeV using OBEP models fitted to the most recent phase-shift data. We have presented three basic models, plus a number of variations. Model I, which includes contributions from $\pi\pi$ scattering data, is in better harmony with the latest N-N data than with earlier N-N phase-shift data. The model is very realistic, with only coupling constants and form factor parameters taken to be adjustable parameters. Because of the realism of the model, the resulting potentials should be useful for a wide range of applications. Model II is made primarily to fit the data in the low-energy region, that is, the scattering data at 0–200 MeV and the deuteron data and would work best for applications involving low-energy phenomena. Properties such as deuteron D-state probability and triton binding energy are predicted much more accurately by this model than by phenomenological models such as the Hamada-Johnston potential. Model III showed that a much better fit is obtained, particularly at 325 MeV, by modifying the velocity-dependent terms in the potential.

In final conclusion we might reiterate that recent experimental data and analyses reveal some deficiencies in the Livermore X phase parameters, to which most of presently available potentials refer. Our potentials by referring to the new data should represent significant advances. Because of their improved fit to recent phase-shift and deuteron parameters we believe each of these potentials should be appropriate for use in nuclei and nuclear-matter calculations and for examination in other nuclear and particle processes.

The authors would like to thank Dr. R. A. Arndt, Dr. J. A. Edgington, Dr. P. Signell, Dr. R. Hess, and Dr. D. H. Fitzgerald for making available prepublication copies of their recent data or phase-shift analyses. Computer time for the numerical calculations in this work was provided by the Research Council of the University of Florida.

APPENDIX: DATA FOR THE χ^2 TEST

The χ^2 value is defined by $\chi^2=\sum[(\delta^i_{\rm th}-\delta^i_{\rm ex})/\Delta^i_{\rm ex}]^2$, where $\delta^i_{\rm th}$, $\delta^i_{\rm ex}$, and $\Delta^i_{\rm ex}$ are the theoretical and experimental phase parameters and the experimental error bars, respectively. The χ^2 tests for the models in Secs. IV and V are made for 72 pieces of data at 25, 50, 100, 150, 200, and 325 MeV for the phase parameters with $J=0$, 1, and 2. At 50 MeV we use the data by Arndt[22] except ϵ_1 and $\delta(^1P_1)$. For these two we use the combined data of Arndt[22] and Signell.[21] The procedure of the combination is as follows. Suppose two data as $X_1 \pm\Delta_1$ and $X_2\pm\Delta_2$; then for the combination $X\pm\Delta$ are defined by

$$X=\tfrac{1}{2}(\max\{X_1+\Delta_1,X_2+\Delta_2\}+\min\{X_1-\Delta_1,X_2-\Delta_2\}),$$

$$\Delta=\tfrac{1}{2}(\max\{X_1+\Delta_1,X_2+\Delta_2\}-\min\{X_1-\Delta_1,X_2-\Delta_2\}).$$

At 325 MeV we use the combined data of the Arndt[22] and Edgington[18] based on the most recent experiment at TRIUMPH. This χ^2 test is called a χ^2_C test.

In Sec. III a χ^2 test (in which the χ^2 data are Arndt's[22] energy-independent solution at 25, 50, 100, 150, 200, and 325 MeV) is used to test model I. These data differ only from AHR[15] at 50 and 325 MeV. This test is denoted by χ^2_A test.

We also use in model II′ the χ^2 data given by the energy-dependent solution in AHR.[15] This is called a $\chi^2_{\rm AHR}$ test.

---

*On leave from Osaka University, Osaka, Japan.

[1]A. E. S. Green, Phys. Rev. 73, 519 (1948); 75, 1926 (1949); 76, L870, A460 (1949); and (unpublished).
[2]S. Sawada, T.Ueda, W. Watari, and M. Yonezawa, Prog. Theor. Phys. 28, 991 (1962); 32, 380 (1964).
[3]S. Ogawa, S. Sawada, T. Ueda, W. Watari, and M. Yonezawa, Prog. Theor. Phys. Suppl. 39, 140 (1967).
[4]A. E. S. Green and R. D. Sharma, Phys. Rev. Lett. 14, 380 (1965); A. E. S. Green, T. Sawada, and R. D. Sharma, *Isobaric Spin in Nuclear Physics* (Academic, New York, 1966).
[5]A. E. S. Green and T. Sawada, Nucl. Phys. B2, 276 (1967); Rev. Mod. Phys. 39, 594 (1967).

[6]T. Ueda and A. E. S. Green, Phys. Rev. 174, 1304 (1968); Nucl. Phys. B10, 289 (1969).
[7]A. E. S. Green, F. Riewe, M. L. Nack, and L. D. Miller, in *Proceedings of the International Symposium on the Present Status and Novel Developments in the Nuclear Many-Body Problem, Rome, September, 1972,* edited by F. Calogero and C. Ciofi Degli Atti (Editrice Compositori, Bologna, 1973).
[8]T. Ueda, see Ref. 7, p. 1.
[9]A. Gersten, R. H. Thompson, and A. E. S. Green, Phys. Rev. D 3, 2069, 2076 (1971).
[10]A. E. S. Green, M. H. MacGregor, and R. Wilson, Rev. Mod. Phys. 39, 495–715 (1967); D. F. Measday, Second International Conference on the Nucleon-Nucleon Interaction, Vancouver, British Columbia June 27–30, 1977 [American Institute of Physics, New York (to be published)].
[11]T. Ueda, M. Nack, and A. Green, Phys. Rev. C 8, 2061 (1973).
[12]S. Furuichi, Prog. Theor. Phys. Suppl. 39, 190 (1967); H. Partovi and E. Lomon, Phys. Rev. D 2, 1999 (1970).
[13]M. Nack, T. Ueda, and A. Green, Phys. Rev. D 10, 3617 (1974).
[14]R. W. Stagat, F. Riewe, and A. E. S. Green, Phys. Rev. Lett. 24, 631 (1970); Phys. Rev. C 3, 552 (1971); F. E. Riewe, M. L. Nack, and A. E. S. Green, *ibid.* 10, 2210 (1974).
[15]R. A. Arndt, R. H. Hackman, and L. D. Roper, Phys. Rev. C 15, 1002 (1977).
[16]R. E. Seamon, K. A. Friedman, G. Breit, R. D. Haraeg, J. M. Holt, and A. Prakash, Phys. Rev. 165, 1579 (1968).
[17]M. H. MacGregor, R. A. Arndt, and R. M. Wright, Phys. Rev. 182, 1714 (1969).
[18]J. A. Edgington, in Proceedings of the Second International Conference on the Nucleon-Nucleon Interaction (see Ref. 10).
[19]D. Besset *et al.*, in Proceedings of the Second International Conference on the Nucleon-Nucleon Interaction (see Ref. 10).
[20]D. H. Fitzgerald *et al.*, in Proceedings of the Second International Conference on the Nucleon-Nucleon Interaction (see Ref. 10).
[21]P. Signell (unpublished).
[22]R. A. Arndt, in Proceedings of the Second International Conference on the Nucleon-Nucleon Interaction (see Ref. 10).
[23]W. Ochs, in Proceedings of the Second International Conference on the Nucleon-Nucleon Interaction (see Ref. 10).
[24]T. Janssens, R. Hofstadter, E. B. Hughes, and M. R. Yearian, Phys. Rev. 142, 922 (1966); M. Goitein, J. R. Dunning, and R. Wilson, Phys. Rev. Lett. 18, 1018 (1967).
[25]J. P. Baton, G. Laurens, and J. Reignier, Phys. Lett. 33B, 525, 528 (1970).
[26]A. Gersten and A. E. S. Green, Phys. Rev. 176, 1199 (1968).
[27]S. C. C. Ting, in *Proceedings of the Fourteenth International Conference on High Energy Physics, Vienna, 1968,* edited by J. Prentki and J. Steinberger (CERN, Geneva, 1968), p. 43.
[28]S. R. Deans and W. G. Holladay, Phys. Rev. 165, 1886 (1968).
[29]P. M. Preedom *et al.*, Phys. Lett. 65B, 31 (1976).
[30]L. M. Delves, in *Few-Body Problems in Nuclear and Particle Physics,* proceedings of the Quebec, Conference, 1974, edited by R. J. Slobodrian, B. Cujec, and K. Ramavataram (Univ. of Laval Press, Quebec, Canada, 1975), p. 446.
[31]C. W. Wong and T. Sawada, Ann. Phys. (N.Y.) 72, 107 (1972).
[32]A. E. S. Green and N. A. Engler, Phys. Rev. 91, 40 (1953).
[33]T. Ueda, T. Sawada, and S. Takagi, Nucl. Phys. A285, 429 (1977).
[34]T. Ueda and S. Takagi, Prog. Theor. Phys. 58, 3 (1977).
[35]T. Ueda and A. E. S. Green (unpublished).
[36]K. Holinde and R. Machleidt, Nucl. Phys. A256, 479 (1976).
[37]T. Ueda, Prog. Theor. Phys. 47, 572 (1972); 48, 2276 (1972).